# Domain walls and domain wall resistivities in CoxPd1–x(111) and CoxPt1–x(111)

Peter Weinberger


# Domain walls and domain wall resistivities in $Co_xPd_{1-x}(111)$ and $Co_xPt_{1-x}(111)$

| | |
|---|---|
| Journal: | *Philosophical Magazine & Philosophical Magazine Letters* |
| Manuscript ID: | TPHM-08-Nov-0430.R1 |
| Journal Selection: | Philosophical Magazine |
| Date Submitted by the Author: | 13-Dec-2008 |
| Complete List of Authors: | Weinberger, Peter; Center for Computational Nanoscience |
| Keywords: | domain structure, resistivity |
| Keywords (user supplied): | |

Note: The following files were submitted by the author for peer review, but cannot be converted to PDF. You must view these files (e.g. movies) online.

smith-4a.tex

# Domain walls and domain wall resistivities in $Co_xPd_{1-x}(111)$ and $Co_xPt_{1-x}(111)$

P. Weinberger
Center for Computational Nanoscience
Seilerstätte 10/22, A-1010 Vienna, Austria

December 13, 2008

**Abstract**

In using the relativistic Screened Korringa-Kohn-Rostoker method and a multi-scale approach based on a parametrization of the Ginzburg-Landau expansion of the free-energy as a functional of the magnetization density, domain wall widths in $Co_xPd_{1-x}$ and $Co_xPt_{1-x}$ are determined by considering these substitutionally disordered alloys as two-dimensionally invariant systems. It is shown that in $Co_xPd_{1-x}$ domains are formed nearly over the whole concentration range, while in $Co_xPt_{1-x}$ domain wall formation only occurs near 50% Co and for Co rich alloys. Based on these results resistivities in the presence and absence of domains walls are evaluated in terms of the relativistic Kubo-Greenwood equation. In contrast to $Co_xNi_{1-x}$, it turns out that both systems are unsuitable as race track materials.

## 1 Introduction

The (bulk) phase diagram of $Co_xPd_{1-x}$ [1] shows no ordered phases: Co and Pd form a continuous series of fcc solid solutions with complete solubility at all compositions. The phase diagram of $Co_xPt_{1-x}$ [1] on the other hand exhibits two superstructures, namely at $x = 0.25$ and 0.5, but otherwise seems to be statistically disordered on an fcc lattice. Co/Pd and Co/Pt are well-studied systems in the literature with available investigations ranging from typical bulk studies [2] - [5], fee surfaces of Co on Pd and Pt [6], (phenomenological) micromagnetic studies of magnetization switching [7] - [10], ab initio attempts thereof [11], small Co clusters or nanostructures on top of Pt [13] - [15], ab initio descriptions of magneto-optical properties [16] - [17], to attempts to measure and characterize domain wall resistivities [18].

Studies of domain walls in nano-wires and their resistivities suddenly became very prominent once the idea of race track memories was coined, namely the suggestion to use current driven domain wall motions as an underlying physical

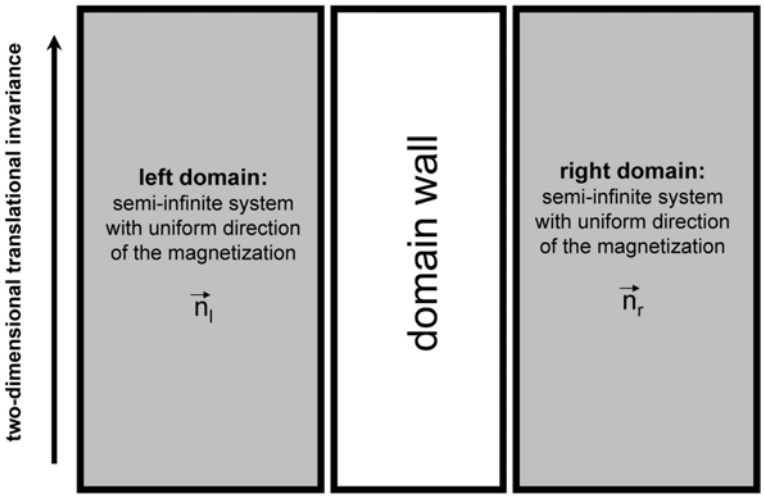


Figure 1: Schematic view of a 180° domain wall.

principle for a completely new type of solid state memory devices [19] - [24]. This idea caused a series of theoretical investigations dealing with exactly the set-up used in the experimental studies [25] - [28], partially performed in the hope to suggest other systems [27, 28] than permalloy [25, 26]. In this context also the present paper has to be seen, namely as an attempt to learn more about domain wall formation in $Co_xPd_{1-x}$ and $Co_xPt_{1-x}$ and to find out whether at least one of these systems could serve as a race track material.

# 2 Formal concepts and computational details

## 2.1 Magnetic configurations and domain wall formation energies

In principle the orientations of the magnetization in an infinite layered system characterized by two-dimensional translational invariance (one atom per unit cell), see Fig. 1, are defined by the following set of unit vectors

$$C = \{\vec{n}_l, \vec{n}_1, \vec{n}_2, \ldots, \vec{n}_i, \ldots, \vec{n}_L, \vec{n}_r\} \quad , \tag{1}$$

where $\vec{n}_l$ refers to the uniform direction of the magnetization in the left domain (semi-infinite system), $\vec{n}_r$ to that in the right domain (semi-infinite system) and the $\vec{n}_i$ to those in the $L$ atomic layers forming the domain wall. Eq. (1) specifies a typical non-collinear magnetic configuration in layered system corresponding to a simple parent lattice. There are two special cases, namely $C_0$,

$$C_0 : \vec{n}_l = \vec{n}_r = \vec{n}_i = \vec{z} \quad , \quad i = 1, L \quad , \tag{2}$$

in which the magnetization in all atomic layers of the system points along the surface normal ($\vec{z}$), and $C_1$,

$$C_1 : \vec{n}_l = \vec{n}_r = \vec{n}_i = \vec{x} \quad , \quad i = 1, L \quad , \tag{3}$$

referring to a uniform orientation of the magnetization along the in-plane $\vec{x}$ axis. $C_0$ and $C_1$ are of course so-called collinear magnetic configurations. In principle in the domain wall the $\vec{n}_i$ can vary in an arbitrary manner implying that for a given $L$ the total energy of the whole system has to be minimized with respect to all possible non-collinear arrangement in the domain wall in order to determine the most favorable configuration. Since such a procedure usually is computationally not feasible, a model for the orientations in the various atomic layers in the domain wall is adopted. Here the below scheme for a 180° domain wall is applied

$$\begin{aligned} C_d : \vec{n}_l = \vec{z} \quad , \quad \vec{n}_r = -\vec{z} \quad , \quad \vec{n}_i = \mathbb{D}(\Phi_i)\vec{y} \quad , \\ \Phi_i = 180 i/L \quad , \quad i = 1, L \quad , \end{aligned} \tag{4}$$

that describes a quasi-continuous change of the orientation of the magnetization from $\vec{z}$ to $-\vec{z}$. In Eq. (4) $\mathbb{D}(\Phi_i)$ is the three-dimensional representative of a rotation around the $\vec{y}$ axis (perpendicular to $\vec{x}$ and $\vec{z}$) by an angle $\Phi_i$.

In using the so-called magnetic force theorem the domain wall formation energy at a given value of $L$ is then defined by the difference in the grand potentials between configurations $C_d$ and $C_0$,

$$E(L, x) = E(L, x, C_d) - E(L, x, C_0) \tag{5}$$

$$= \sum_{p=1}^{N} \left( E^p(L, x, C_d) - E^p(L, x, C_0) \right) \quad , \tag{6}$$

where $x$ is the concentration, $p$ denotes atomic layers, and $N$ includes a sufficient number $m$ of "buffer" atomic layers in the left and right domain in order to guarantee a smooth transition between the domain wall and its adjacent domains,

$$N = L + 2m \quad . \tag{7}$$

The layer-resolved contributions $E^p(L, x, C_i)$ to the grand potential are given by

$$E^p(L, x, C_i) = \int_{E_b}^{E_F} n^p(L, x, C_i, z)(z - E_F) dz \quad , \tag{8}$$

where $n^p(L, x, C_i, z)$ is the density-of-states of the $p$-th atomic layer in a domain wall of width $L$ corresponding to a magnetic configuration $C_i = C_0, C_1$ or $C_d$. In Eq. (8) $z = \epsilon + i\delta$ is a in general complex energy, $E_b$ the valence band bottom and $E_F$ the Fermi energy. It should be noted that Eq. (5) implies that for $E(L, x) > 0$ configuration $C_d$ (domain wall formation) is preferred, while for $E(L, x) \leq 0$ configuration $C_0$ is the stable one (the system forms a single domain with the direction of the magnetization pointing uniformly along $\vec{z}$).

Since the minimum in $E(L, x)$ with respect to $L$,

$$\left.\frac{dE(L,x)}{dL}\right|_{L_0} = 0 \quad , \tag{9}$$

usually occurs at rather large values of $L$, it was suggested [29] to cast the Ginzburg-Landau expansion of the (generalized) free-energy as a functional the magnetization density into a multi-scale approach, since then the $E(L, x)$ can be formulated in terms of two constants $a(x)$ and $b(x)$,

$$E(L, x) = A(x)\left(\frac{a(x)}{L} + b(x)L\right) \quad , \tag{10}$$

the first one being the so-called exchange, the second one the anisotropy energy parameter. The equilibrium width of the domain wall for a given concentration $x$ is then simply given by

$$L_0(x) = +\sqrt{a(x)/b(x)} \quad . \tag{11}$$

It should be noted that since $E(L, x)$ is quadratic in $L$, in principle the value of $E(L, x)$ needs to be determined only at two (large enough) values of $L$ in order to evaluate $L_0(x)$. The above described multi-scale approach was rigorously tested [29] and successfully applied to permalloy [25, 27], [28] and $Co_xFe_{1-x}$ and $Co_xNi_{1-x}$ [26].

## 2.2 Sheet resistances and resistivities

In principle for a particular magnetic configuration $C_i$ the current perpendicular to the planes of atoms ($CPP$) defined over a certain length $L$ is given by [30]

$$\rho_{CPP}(L, x, C_i) = \frac{1}{L}\int\!\!\int_{-\infty}^{\infty} \rho(z, z'; x, C_i) dz dz' \ , \tag{12}$$

and the corresponding sheet resistance by

$$r(L, x, C_i) = L\rho_{CPP}(L, x, C_i) \ . \tag{13}$$

For large enough $L$ the resistivity $\rho_{CPP}(L, x, C_i)$ can be obtained from the $zz$-component of the conductivity tensor, $\sigma_{zz}(L, x, C_i)$,

$$\rho_{CPP}(L, x, C_i) \sim \rho_{zz}(L, x, C_i) = \sigma_{zz}^{-1}(L, x, C_i) \ . \tag{14}$$

As it is virtually impossible to calculate the conductivity tensor by means of ab initio methods for very large $L$ one can make use of the fact that $r(L, x, C_i)$ is linear in $L$,

$$r(L, x, C_i) = L\rho_{zz}(L, x, C_i) = \alpha(x, C_i) + \beta(x, C_i)L \ , \tag{15}$$

which, furthermore, has the useful limiting properties

$$0 < c < 1 : \lim_{L\to\infty} \rho_{zz}(L, x, C_d) = \beta(x, C_d, c) = \rho_{zz}(x, C_0) \ , \tag{16}$$

$$c = 0, 1 : \lim_{L\to\infty} \rho_{zz}(L, x, C_d) = \rho_{zz}(C_0) = 0 \ . \tag{17}$$

In Eq. 16 $\rho_{zz}(x, C_0)$, $0 < x < 1$, is the $zz$-component of the residual ("bulk") resistivity corresponding to configuration $C_0$, see Eq. (2). As is well-known for pure systems ($c = 0, 1$) the constant $\beta(C, c)$ has to be exactly zero. Eq. (17) can therefore be used to check the accuracy of the applied numerical procedure, in particular, since $\rho_{zz}(L, x, C_i)$ is evaluated by means of an analytical continuation of resistivities defined for complex Fermi energies.[32]

# 3 Numerical details

All *ab initio* calculations for $Co_xPd_{1-x}(111)$ and $Co_xPt_{1-x}(111)$ were performed at the experimental lattice constant using Vegard's law, e.g.,

$$a_0(x) = xa_0(Co) + (1 - x)a_0(Pd)$$

(Co: 6.5509, Pd: 7.3530, Pt: 7.4137 [a.u.]) in terms of the spin-polarized (fully) relativistic screened Korringa-Kohn-Rostoker (SPR-KKR) method within the frame-work of the inhomogeneous Coherent Potential Approximation. [31] It should be noted that Vegard's law describes rather very well the variation of the experimental lattice parameter of $Co_xPd_{1-x}$ and $Co_xPt_{1-x}$ with respect to the concentration. [1]

In using the selfconsistent potentials and exchange fields corresponding to configuration $C_0$ the grand potentials $E(L, x)$, see Eq. (5), were evaluated by means of a contour integration along a semi-circle using a 16 point Gaussian-quadrature and 1830 $k$ points per irreducible part of the surface Brillouin zone (ISBZ). The equilibrium domain wall width was then determined at $L = 222$ and 324 [ML]. For an extensive discussion of the accuracy of the fit based on Eq. (10) using the same numerical parameters, see Ref. [25].

The electric transport properties were evaluated at complex Fermi energies by means of the fully relativistic Kubo-Greenwood equation [32] using also 1830 $k$ points per ISBZ and then analytically continued to the real axis. All resistivities at $L_0$ and $L = \infty$ (bulk) were determined via Eq. (15) using the calculated values of $r(L, x, C_i)$ at $L = 60$ and 120 [ML]. A detailed study of the numerical properties of Eq. (15) is to be found in Ref. [33], in which not only the $L$ dependence is discussed but also the accuracy of the analytical continuation

to the real axsis. It should be noted that for both fits, namely employing Eqs. (10) and (15), sufficiently large values of $L$, well separated from each other, were used in order to exclude any kind of "neighborhood effects". For computational reasons the two values had to be smaller in the case of the electric properties. However, in principle – as was already mentioned and was amply discussed in Refs. [25, 33] – for these fits an arbitray pair of values of $L$ can be chosen. In both types of calculations the number of "buffer layers", see Eq. (7), was three.

Since a (111) stacking sequence was chosen for both systems, the equilibrium domain wall width in [nm] and the unit area in $[\mathrm{nm}]^2$ is defined by

$$L_0\ [\mathrm{nm}] = \frac{a_0(x)}{\sqrt{3}} L \quad , \quad A(x) = \frac{\sqrt{3} a_0^2(x)}{4}\ [\mathrm{nm}]^2$$

where $L$ is the number of atomic layers at which Eq. (9) is fullfilled.

# 4 Discussion of results

## 4.1 Spin and orbital moments

As already stated in the introduction, the bulk systems $\mathrm{Co}_x\mathrm{Pd}_{1-x}$ and $\mathrm{Co}_x\mathrm{Pt}_{1-x}$ are well-studied in the literature, and yet surprising features are found when they are directly compared to each other. In Fig. 2 the spin and orbital moments of Co and Pd (Pt) are shown versus the concentration $x$. As can be seen the spin moments in the two substitutionally disordered systems are very much alike. There are hardly any differences in the Co spin moment whether Co is alloyed with Pd or Pt. Also the induced spin moments for Pd and Pt are very similar in value through the whole studied concentration range. However, the orbital moments behave completely different: with decreasing Co content in $\mathrm{Co}_x\mathrm{Pd}_{1-x}$ the Co orbital moments increase substantially while in $\mathrm{Co}_x\mathrm{Pt}_{1-x}$ they decrease. Taking for example the values at $x = 0.25$ the difference is about 0.07 [$\mu_B$]. This *per se* is quite a big value for an orbital moment! Also the induced orbital moments at Pd or Pt sites are remarkably different. For large Co concentrations they differ by nearly a factor two.

## 4.2 Domain wall formation energies & domain wall widths

Turning now to the domain wall formation energies, see Eq. (5), displayed in Fig. 3 for $L = 222$ and $L = 324$, it seems that two completely different systems are dealt with, in particular since in the case of $\mathrm{Co}_x\mathrm{Pt}_{1-x}$ the domain wall energy for $L = 324$ is negative for $x < 0.4$ and $0.6 < x < 0.9$. From Eq. (5) – as should be recalled – follows directly that in these concentration ranges the magnetic configuration $C_0$ is preferred, i.e., the magnetization is uniformly aligned in all atomic layers of the system along the surface normal. This of course implies that no domains and therefore domain walls are formed.

It is interesting to explore from which parts in a domain wall of given width the main contributions to the domain wall formation energy arise. In order to

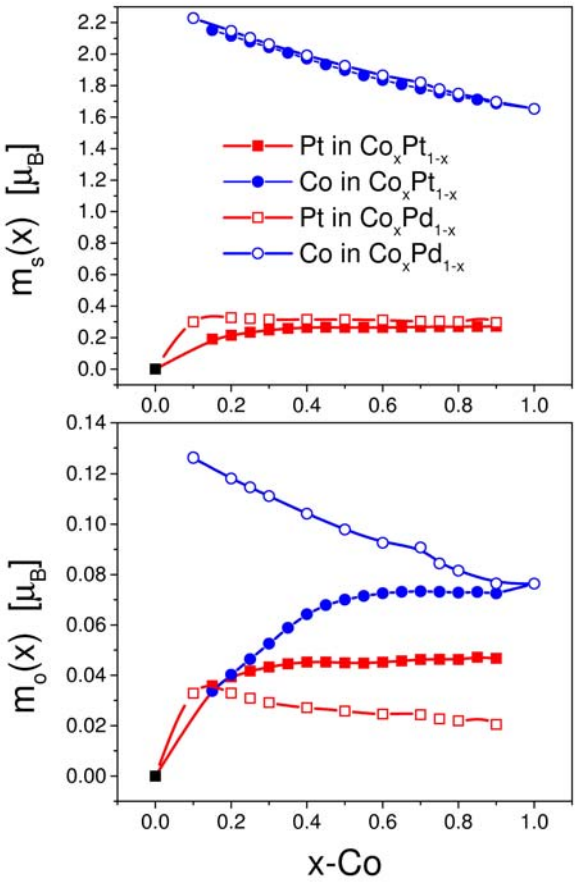


Figure 2: Spin and orbital moments in fcc $Co_xPd_{1-x}(111)$ and fcc $Co_xPt_{1-x}(111)$.

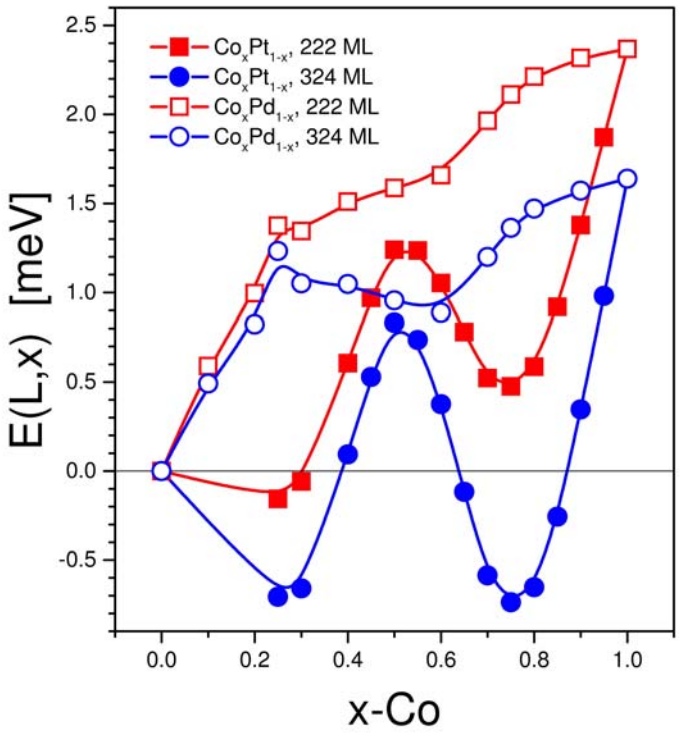


Figure 3: Domain wall formation energies in fcc $Co_xPd_{1-x}(111)$ and fcc $Co_xPt_{1-x}(111)$.

illustrate corresponding changes with respect to the concentration in Fig. 4 the layer-resolved quantities, see Eqs. (5) and (6), are displayed for $L = 324$ and $x = 0.1, 0.3$ and $0.5$ in the case of $Co_xPd_{1-x}$. Quite obviously these layer-resolved domain wall energies vary rapidly at the very beginning and end of the domain wall. In the lower part of this figure this particular feature is shown for the first 10 atomic layers. As can be seen the rise to a certain value occurs within the first five layers.

In the interior of a domain wall the layer-resolved domain wall formation energies vary differently for different concentrations. For example at $x = 0.5$ there is a minimum in the middle of the domain wall, while for $x = 0.3$ a maximum is present. In the middle of a domain wall the orientation of the magnetization is perpendicular to the ones in the adjacent domains, indicating a higher ($Co_{30}Pd_{70}$) or lower ($Co_{50}Pd_{50}$) contribution to the in-plane anisotropy of the respective atomic layers. In the case of $Co_{10}Pd_{90}$ even two maxima, occur separated symmetrically by a minimum in the middle of the wall. From Fig. 4 follows that obviously the "interface" of the domain wall with its adjacent domains is of crucial importance, a fact that most likely will have to enter an *ab initio* description of domain wall motions. In Fig. 5 for $Co_{50}Pd_{50}$, $L = 324$, the contributions of the components Co and Pd to the domain wall formation energy are depicted. As can be seen the contribution from Pd is surprisingly large in particular in the middle of the domain wall.

To illustrate the variation of $E(x, L)$ with $L$, in Fig. 6 a few characteristic cases are shown for $Co_xPd_{1-x}$. It should be noted that in this figure deliberately $L$ is given in units of [ML] in order to prove the usefulness of Eq. (10). From this figure it can be seen that for $x = 0.9$ the minimum is very shallow, while for $x = 0.1$ it is reasonably deep. In all cases the actual equilibrium domain wall formation energy is rather small, namely less than about 50 [$\mu$eV]. The parameters for the fit, the exchange and the anisotropy energy, are displayed together with the equilibrium domain wall width in Fig. 7. In particular from this figure the enormous differences between $Co_xPd_{1-x}$ and $Co_xPt_{1-x}$ become transparent that were already present when discussing the orbital moments. With the exception of very dilute alloys of Co with Pd, over the whole concentration range in $Co_xPd_{1-x}$ $180^0$ domains are formed. The width of these domain walls is surprisingly small for $x < 0.3$ and $0.5 < x < 0.7$. Because of the minimum in the anisotropy parameter at about $x = 0.4$ the domain wall width at this concentration becomes rather large, in the same manner as a decreasing anisotropy for high Co concentrations causes a steady increase of the domain wall width. This behavior follows directly from Eq. (11) since the anisotropy parameter serves as denominator.

For $Co_xPt_{1-x}$ the situation is completely different, since, as was already said, for $x < 0.4$ and $0.6 < x < 0.9$ the domain wall formation energies are negative causing the exchange parameter in Eq. (11) to vanish. These are the concentration regimes in which no domain wall formation occurs. For $x > 0.9$ both the exchange as well as the anisotropy parameter vary rapidly. It seems that the anisotropy parameter is increasing in order to overcome the fast decline in the exchange parameter. Consequently in this concentration regime

the equilibrium width changes very fast with the concentration, being very small indeed for $x = 0.9$.

### 4.3 Domain wall resistivities

Nowadays the main interest in domain walls is of course directed to their resistivities, in particular to the change in the anisotropic magnetoresistance (AMR) of statistically disordered system in the presence

$$AMR(L_0, x) = \frac{\rho_{zz}(L_0, x, C_d) - \rho_{zz}(L_0, x, C_1)}{\rho_{zz}(L_0, x, C_d)} \tag{18}$$

and absence

$$AMR(x) = \frac{\rho_{zz}(x, C_0) - \rho_{zz}(x, C_1)}{\rho_{zz}(x, C_0)} \tag{19}$$

of a domain wall. Race track memories, for example, are based on the fact that $AMR(L_0, x) - AMR(x) < 0$.

Clearly, in order to evaluate such a difference, it is necessary to evaluate first the equilibrium domain wall width $L_0$ via Eq. (10) and only then $\rho_{zz}(L_0, x, C_d)$ and $\rho_{zz}(L_0, x, C_1)$ by making use of Eqs. (13) - (16). In Fig. 8 $\rho_{zz}(L_0, x, C_d)$, $\rho_{zz}(L_0, x, C_1)$, $\rho_{zz}(x, C_0)$ and $\rho_{zz}(x, C_1)$ in $Co_xPd_{1-x}$ and $Co_xPt_{1-x}$ are displayed versus the concentration $x$. As one can see, although in the presence of a domain wall (whenever it exists) the resistivity is increased, however, the differences between $\rho_{zz}(L_0, x, C_d)$ and $\rho_{zz}(L_0, x, C_1)$ are just as small as in the "bulk" case, i.e., between $\rho_{zz}(x, C_0)$ and $\rho_{zz}(x, C_1)$. In terms of race track memories these two system are therefore totally uninteresting, since the AMR is of the order of 1 - 2% and therefore the difference $AMR(L_0, x) - AMR(x)$ becomes uninteresting. Only in those cases in which the domain wall width is rather small such as for example in $Co_{25}Pd_{75}$ a reduction of the AMR of about 2% caused by the presence of a domain wall might turn out to be sufficient because of the possibility of a substantial miniaturization of devices, or because other materials properties become relevant in technological applications.

The results for $\rho_{zz}(x, C_0)$ and $\rho_{zz}(x, C_1)$ (absence of a domain wall) are very similar indeed to those obtained by Ebert et al. [34] using also the relativistic Kubo-Greenwood equation, however, in the context of three-dimensional cyclic boundary conditions and by integrating along the real axis. They also found a bulk anisotropic magnetoresistance ratio, see Eq. (19), of about 1%, implying that there is almost no difference in the resistivity whether the orientation of the magnetization is parallel or perpendicular to the direction of the current. In their calculations as well as in the present ones there is a peak in the resistivity at about 20% Co in $Co_xPd_{1-x}$ and at about 30% in $Co_xPt_{1-x}$. The peak values of 14 - 15 [$\mu\Omega\ cm$] in $Co_xPd_{1-x}$ and about 40 [$\mu\Omega\ cm$] in $Co_xPt_{1-x}$ agree rather well with existing experimental data, namely 16 [$\mu\Omega\ cm$] and 35 [$\mu\Omega\ cm$], respectively. For further details, see Ref. [34].

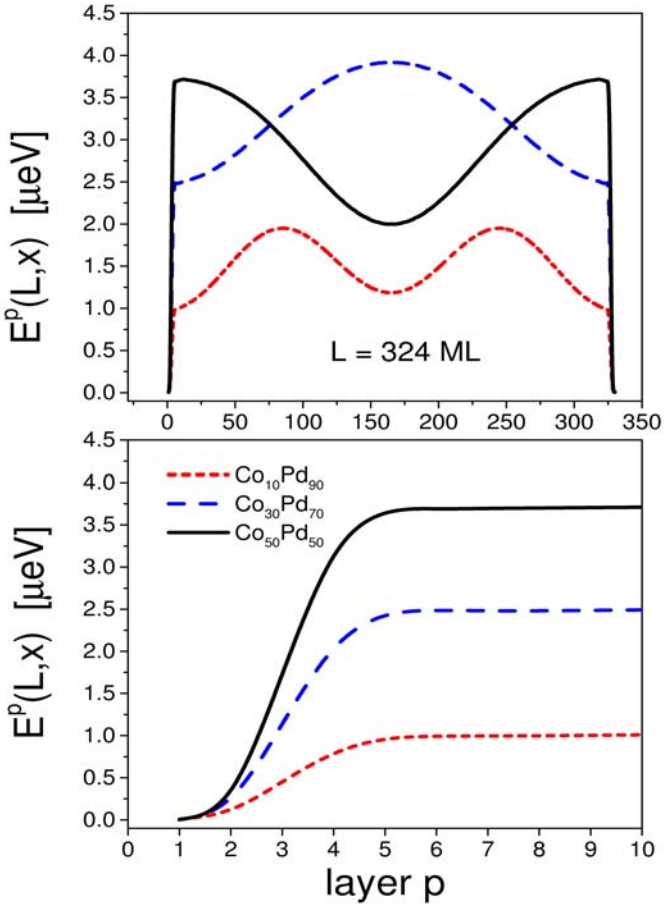


Figure 4: Layer-resolved domain wall formation energies in fcc $Co_xPd_{1-x}(111)$.

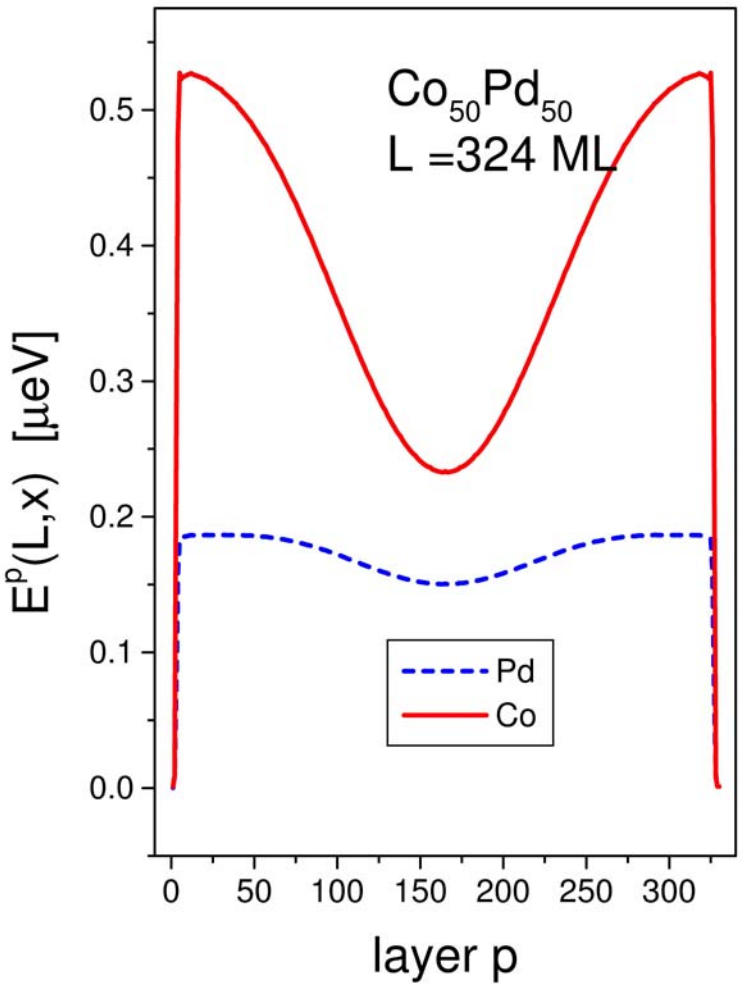


Figure 5: Component and layer-resolved domain wall formation energies in fcc $Co_{50}Pd_{50}(111)$.

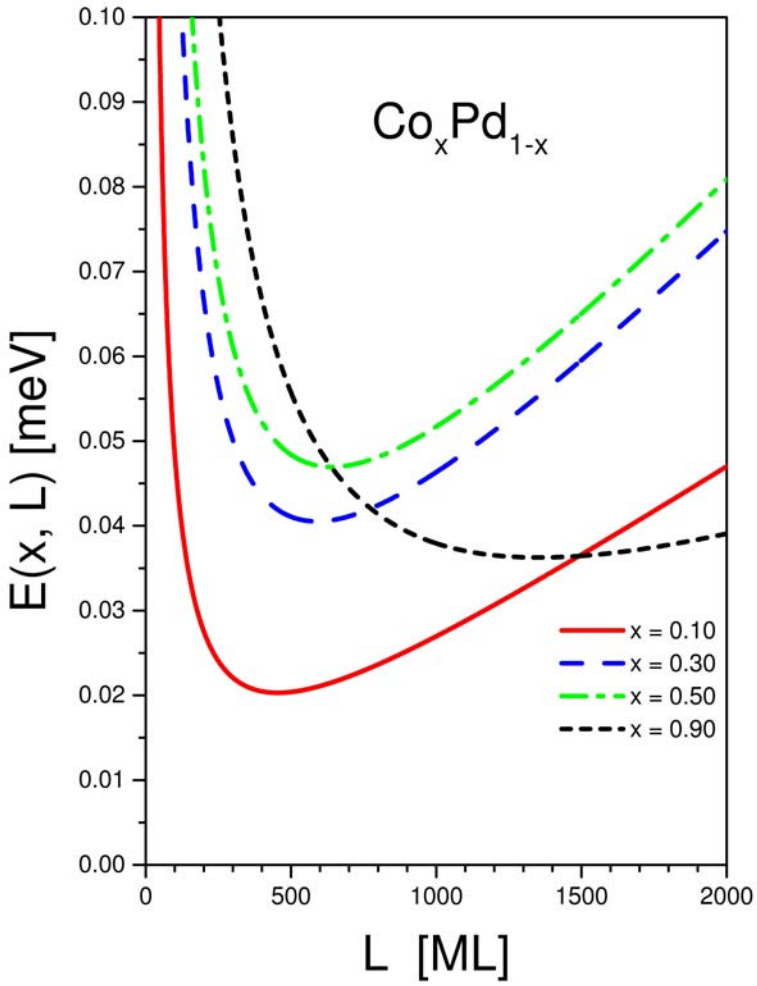


Figure 6: Fitted domain wall formation energies in fcc $Co_xPd_{1-x}(111)$.

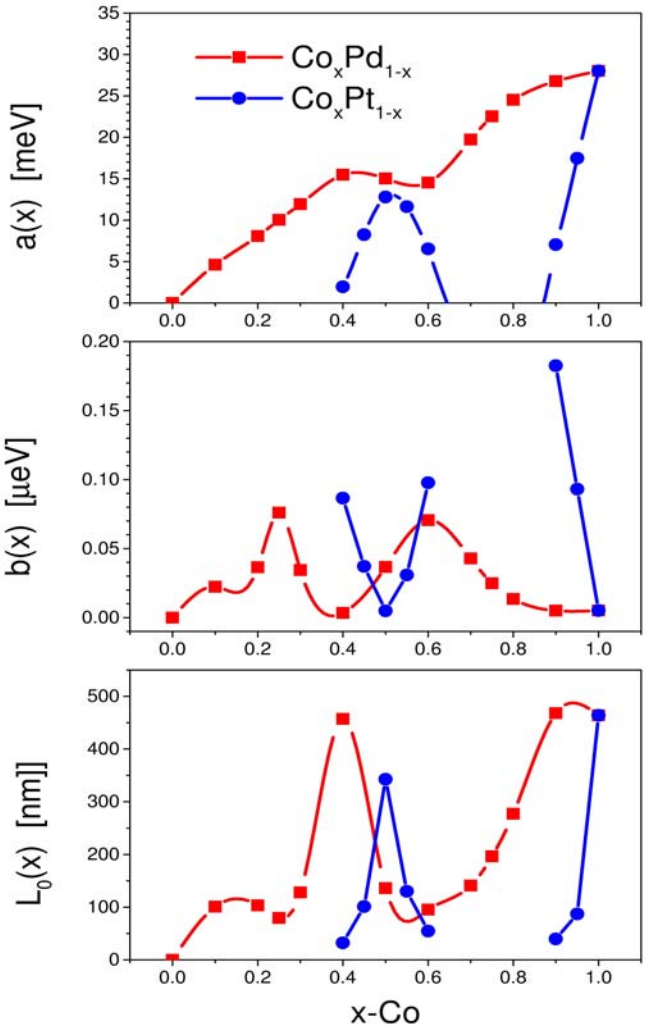


Figure 7: Exchange energy parameter (top), anisotropy parameter (middle) and equilibrium domain wall width in fcc $Co_xPd_{1-x}(111)$ and fcc $Co_xPt_{1-x}(111)$.

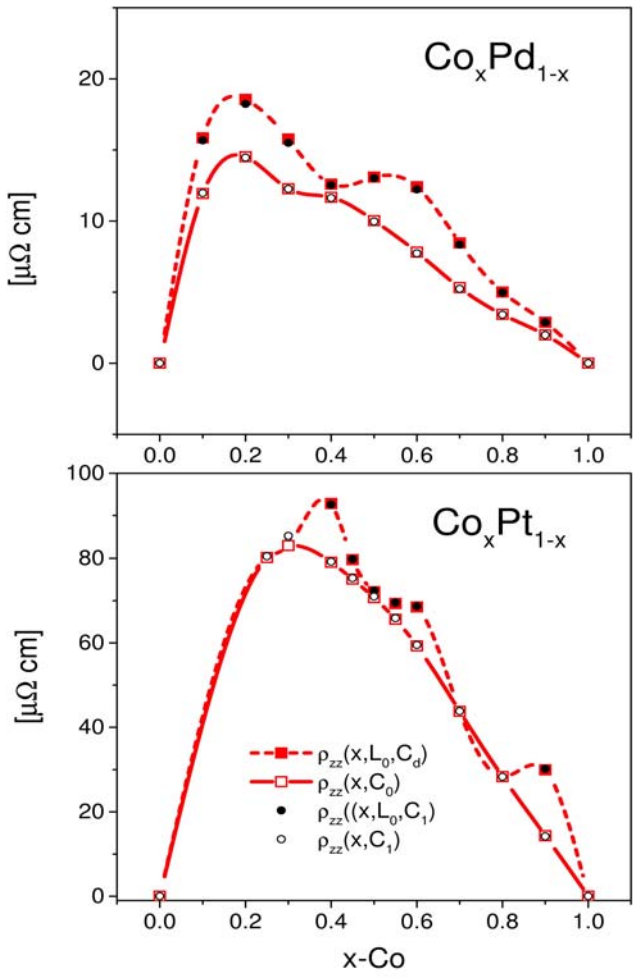


Figure 8: Domain wall and "bulk" resistivities $\rho_{zz}$ in fcc $Co_xPd_{1-x}(111)$ and fcc $Co_xPt_{1-x}(111)$.

## 5 Conclusion

Coming finally back to the phase diagrams for $Co_xPd_{1-x}$ and $Co_xPt_{1-x}$ it is perhaps not surprising that in the case of $Co_xPd_{1-x}$, for which no ordered phases have been found, domain wall formation takes place over the whole concentration range. Only around 40% Co the system tends to large domain wall widths, since the anisotropy energy is sufficiently small. In $Co_xPt_{1-x}$ the two ordered phases behave differently: at about 50% Co, almost as sharp as in the phase diagram (40% - about 65%), a domain wall of width equal to that in pure Co is formed. On the other hand the ordered phase at 25% Co seems to form single domains. It should be noted that also around 75% the phase diagram indicates traces of an ordered phase. In that concentration regime once again only single domains appear to exist.

As far as the resistivity results are concerned, they did not offer new possiblilities in direction of race track memories. Interestingly enough, in the series $Co_xNi_{1-x}$, $Co_xPd_{1-x}$ and $Co_xPt_{1-x}$ only $Co_xNi_{1-x}$ [27] showed a reasonable reduction in the AMR. It seems therefore that for the time being permalloy, $Ni_xFe_{1-x}$, $x \sim 0.85$, is the best possible choice for race track memories. The only improvement that possibly can be made is perhaps the use 90° domains instead of 180° domains. [28]

**Acknowledgement 1** *This paper is dedicated to my friend Jim Smith on account of his 65-th birthday. He not only insisted that I became an associate editor of Philosophical Magazine quite a few years ago, but he also facilitated many enjoyable summers in Los Alamos for me (working in the lab) and my family. After all these extended visits to Los Alamos, New Mexico became as familiar to us as our own home country. Occasionally it is quite appropriate to say thank you!*

## References

[1] Landolt-Börnstein, Springer-Verlag, Berlin, Heidelberg (2008).

[2] Y.S. Shi, M.F. Wang, D.Qian, G.S. Dong, X.F. Jin, and Ding-Sheng Wang, J. Mag. Magn. Mat. **277**, 71 (2004).

[3] A. Kootte, C. Haas and R A de Groott, J. Phys.: Condens. Matter **3**, 1133 (1991).

[4] L. H. Lewis, J. Kim, K. Barmak and D. C. Crew, J. Phys. D: Appl. Phys. **37**, 2638 (2004).

[5] S. D. Willoughby, R. A. Stern, R. Duplessis, and J. M. MacLaren, J. Appl. Phys. **93**, 7145 (2003).

[6] L. Szunyogh, P. Weinberger and C. Sommers, Phys. Rev. B **60**, 11 910 (1999).

[7] Y. S. Lee, J. Y. Rhee, C. N. Whang, and Y. P. Lee, Phys. Rev. B **68**, 235111 (2003).

[8] J Valentin, Th Kleinefeld, and D Weller, J. Phys. D: Appl. Phys. **29**, 1111 (1996).

[9] U. Nowak, J. Heimel, T. Kleinefeld, and D. Weller, Phys. Rev. B **56**, 8143 (1997).

[10] J. Fidler,T. Schrefl, W. Scholz, D. Suess, R. Dittrich, M. Kirschner, J. Mag. Magn. Mat. **272–276**, 641 (2004).

[11] K. D. Belashchenko and V. P. Antropov, Phys. Rev. B **66**, 144402 (2002).

[12] L. Szunyogh, P. Weinberger and C. Sommers, Phys. Rev. B **60**, 11 910 (1999)

[13] B. Lazarovits, L. Szunyogh, and P. Weinberger, Phys. Rev. B **67**, 024415 (2003).

[14] B. Újfalussy, B. Lazarovits, L. Szunyogh, G. M. Stocks, and P, Weinberger, Phys. Rev. B **70**, 100404(R) (2004).

[15] G. M. Stocks, B. Újfalussy, B. Lazarovits, L. Szunyogh, M. Eisenbach, and P. Weinberger, Progress in Materials Science **52**, 371 (2007).

[16] I. Reichl, J. Zabloudil, R. Hammerling, A. Vernes, L. Szunyogh, and P. Weinberger, Phys. Rev. B **73**, 054402 (2006).

[17] A. Vernes, L. Szunyogh, and P. Weinberger, J. Appl. Phys. **91**, 7191 (2002).

[18] B. Leven, U. Nowak, and G. Dumpich, Europhys. Lett. **70**, 803 (2005).

[19] S. S. P. Parkin, M. Hayashi, and L. Thomas, Science **320**, 190 (2008).

[20] M. Hayashi, L. Thomas, R. Moriya, C. Rettner, and S. S. P. Parkin, Science **320**, 209 (2008).

[21] L. Thomas, M. Hayashi, X. Jiang, R. Moriya, C. Rettner, and S. S. P. Parkin, Science **315**, 1553 (2007).

[22] M. Hayashi, L. Thomas, C. Rettner, R. Moriya, Y. B. Bazaliy, and S. S. P. Parkin, Phys. Rev. Lett. **98**, 037204 (2007).

[23] M. Hayashi, L. Thomas, Y. B. Bazaliy, C. Rettner, R. Moriya, X. Jiang, and S. S. P. Parkin, Phys. Rev. Lett. **96**, 197207 (2006).

[24] M. Hayashi, L. Thomas, C. Rettner, R. Moriya, X. Jiang, and S. S. P. Parkin, Phys. Rev. Lett. **97**, 207205 (2006).

[25] P. Weinberger, Phys. Rev. Lett. **98**, 027205 (2007).

[26] P. Weinberger, Proceedings of the MRS Fall Meeting Boston 2008, MRS-I032-I01 (2008).

[27] P. Weinberger, Phys. Rev. Lett. **100**, 017201 (2008).

[28] P. Weinberger, Phys. Rev. B **78**, 172404 (2008).

[29] J. Schwitalla, B. L. Gyorffy, and L. Szunyogh, Phys. Rev. B **63**, 104423 (2001).

[30] see for example, P. M. Levy and I. Mertig, *Theory of Giant Magnetoresistance*, in D. D. Sarma, G. Kotliar, Y. Tokura (Eds.), Advances in Condensed Matter, Vol. 3, Taylor & Francis, London, New York (2002).

[31] J. Zabloudil, R. Hammerling, L. Szunyogh and P. Weinberger, *Electron Scattering in Solid Matter* (Springer Berlin Heidelberg New York, 2004).

[32] for a review see: P. Weinberger, Physics Reports **377**, 281 (2003).

[33] P. Weinberger, L. Szunyogh, C. Blaas, and C. Sommers, Phys. Rev. B **64**, 184429 (2001).

[34] H. Ebert, A. Vernes, and J. Banhart, Phys. Rev. B **54**, 8479 (1996).

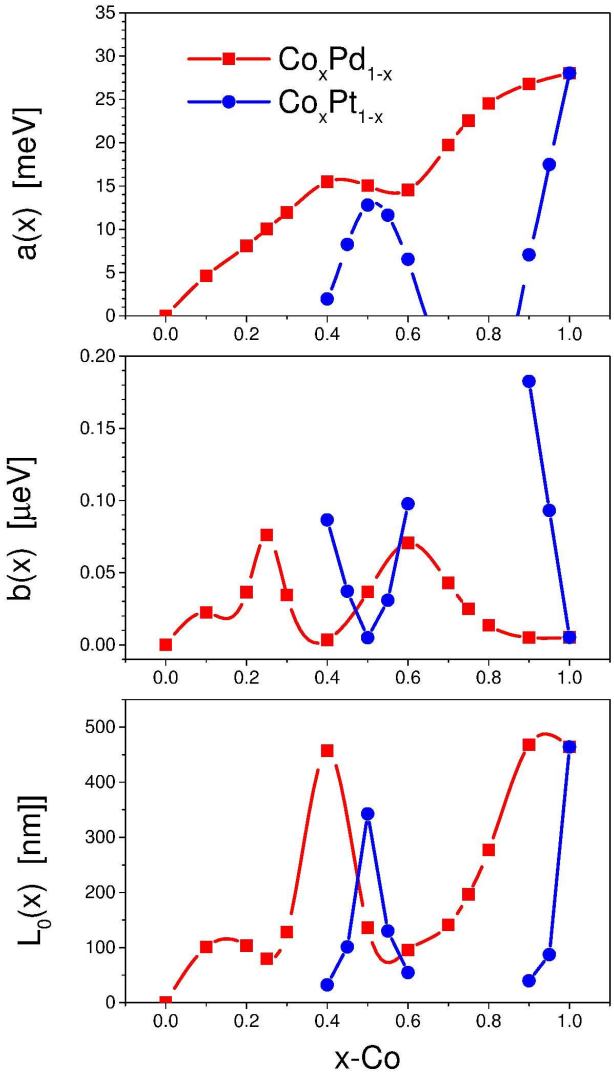


209x297mm (600 x 600 DPI)

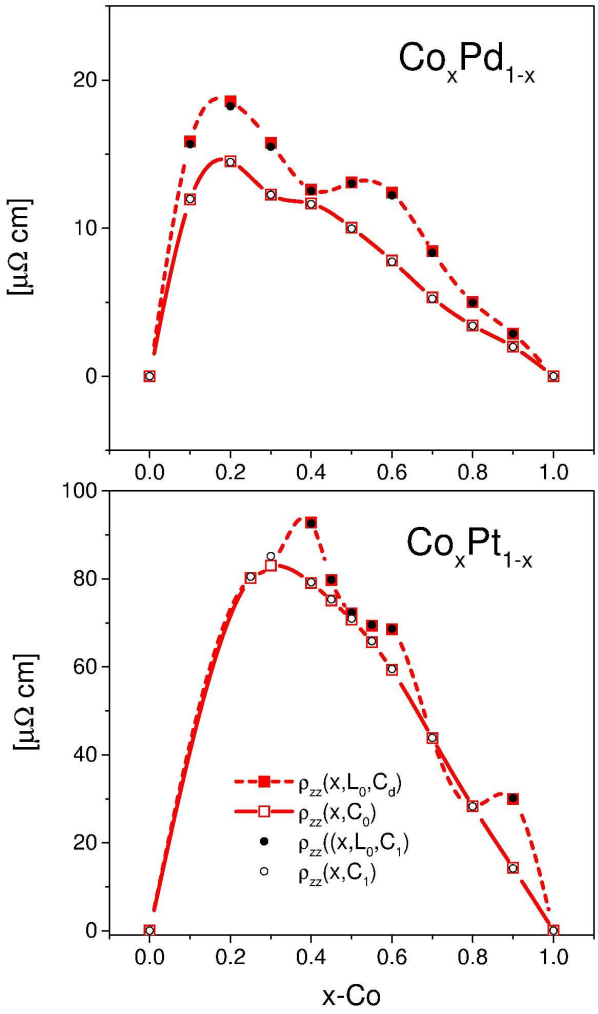


209x297mm (600 x 600 DPI)